Fabrication of Nonperiodic Metasurfaces by Microlens Projection Lithography

Fabrication of Nonperiodic Metasurfaces by Microlens Projection Lithography

Mathieu Gonidec,[1] Mahiar M. Hamedi,[1] Alex Nemiroski,[1] Luis M. Rubio,[1] Cesar Torres,[1] and George M. Whitesides*.[1,2,3]

[1]Department of Chemistry and Chemical Biology, Harvard University, 12 Oxford Street, Cambridge, Massachusetts 02138, United States,

[2]Wyss Institute for Biologically Inspired Engineering, Harvard University, 60 Oxford Street, Cambridge, Massachusetts 02138, United States, and

[3]Kavli Institute for Bionano Science and Technology, Harvard University, 29 Oxford Street, Massachusetts 02138, United States

*Corresponding author, email: gwhitesides@gmwgroup.harvard.edu

ABSTRACT

This paper describes a strategy that uses template-directed self-assembly of μm-scale microspheres to fabricate arrays of microlenses for projection photolithography of periodic, quasiperiodic, and aperiodic infrared metasurfaces. This method of "template-encoded microlens projection lithography" (TEMPL) enables rapid prototyping of planar, multi-scale patterns of similarly shaped structures with critical dimensions down to ~ 400 nm. Each of these structures is defined by local projection lithography, with a single microsphere acting as a lens. This paper explores the use of TEMPL for the fabrication of a broad range of two-dimensional lattices with varying types of non-periodic spatial distribution. The matching optical spectra of the fabricated and simulated metasurfaces confirm that TEMPL can produce structures that conform to expected optical behavior.

MAIN TEXT

Optical metasurfaces – periodic,[1-3] quasiperiodic, or aperiodic[4] patterns of nanoscale metal or dielectric features with subwavelength spacing – enable a degree of engineered control over local and scattered electromagnetic fields not possible with naturally occurring materials.[5] These optically thin materials have the potential to become fundamental components in sensitive chemical and biological sensors[6-11] and flat optics.[12-14] Despite many recent advances, available methods cannot fabricate new designs with the required feature sizes rapidly, or over even moderate areas (~ mm^2 – cm^2). This limitation has slowed the comparison of theory and experiment. This paper describes a method for fabricating infrared metasurfaces that combines the simplicity of self-assembly with the precision of projection lithography to offer new capabilities in the rapid-prototyping of periodic and quasiperiodic metasurfaces, particularly those with feature sizes in the range of 0.4-10 μm.

This method combines two strategies. The first—microlens projection lithography—uses self-assembled arrays of colloidal microlenses that each project an image of a distant, macroscopic mask onto the substrate.[15-17] It enables efficient fabrication of arrays of microstructures (colloidal self-assembly can be rapid), and more importantly, rapid iteration between different masks. The second strategy is to use self-assembled arrays of silica spheres as microlenses, and to template the placement of these spheres. The silica spheres act as lenses with high NA (~ 0.8) and enable spatial resolution down to ~ 0.3 μm. Because the microlenses are small (typically around 5 μm in diameter) and the pattern being projected is large (typically around 5 cm in size) the projected image is greatly reduced in size (~10,000×, relative to the photomask), in a single step. This characteristic relaxes the requirements for the resolution of the photomask to values >1 mm – features easily fabricated by conventional printing or laser-cutting; e-beam or laser writing methods are not required.

The combination of these two strategies—which we call "template-encoded microlens projection lithography" (TEMPL)—overcomes one of the major challenges in fabrication of metasurfaces: rapid evolution in the design of unit cells. TEMPL uses a master template, fabricated by direct-write photolithography, to guide the organization of the silica microspheres into the desired planar arrangement of microlenses. Here, we demonstrate that TEMPL can be used to fabricate periodic and quasiperiodic patterns of identical unit cells, with characteristics necessary for the development of infrared metasurfaces. Although, TEMPL is not suitable for the fabrication of metasurfaces that require changes in the shape of the unit cell, the method is particularly well suited to investigate the influence of the global spatial distribution of "unit cells" on the optical properties of a material. Furthermore, this work demonstrates – for the first time (to our knowledge) – template-directed assembly of micron-scale, complex arrays of spheres coupled with the transfer of these patterns to flat, optically transparent substrates.

In the TEMPL process, a template consisting of cylindrical holes etched in silicon directs the self-assembly of dry, SiO_2 microspheres, which are then transferred to an optically transparent substrate on which they would serve as microlenses for projection lithography. We first prepared a master template by standard direct-write photolithography, followed by reactive ion etching. This step was the most demanding one from the point of view of instrumentation, but can easily be outsourced to commercial vendors. We fabricated cylindrical holes with a width of *c.a.* 95% and a depth of 50% of the diameter of the microspheres. Our method of templating with this master was inspired, in part, by a protocol described by Yoon et al.,[18] which we modified and expanded into a four-step process that yielded consistently reproducible, high-quality patterns. Figure 1a shows a schematic of this procedure. (i) We first selectively filled the wells in the master with polyethyleneimine (PEI), which served as an adhesive for the spheres, by coating the patterned areas of the master with a viscous solution of PEI and then wiping away the excess with a damp, dust-free cloth. This step removed the PEI from the interstitial areas of the master template, while leaving the wells filled. (ii) We then gently rubbed a small amount of dry, monodisperse, silica microspheres onto the master with a clean piece of PDMS. The spheres adhered selectively to the PEI inside the wells; continual rubbing removed excess spheres. Removal of un-templated spheres was aided by carefully introducing a gentle stream of nitrogen. (iii) We next heated the back of the silicon master with a butane torch to burn off the PEI adhesive. At the conclusion of this procedure, the microspheres remained positioned on top of, and centered on the wells, but they no longer adhered to the substrate and were free to be transfered to another surface. Importantly, we chose a hole size slightly smaller than the microspheres to ensure that they did not fall entirely into the holes. (iv) We finally transferred the microspheres to an intermediate surface by placing a thin, flat slab of clean PDMS on top of the microspheres, applying gentle pressure, and peeling the PDMS slab from the master. The

spheres adhered to the PDMS. We found that the most critical steps are the correct cleaning of the excess PEI, and the rubbing of the dry microspheres on the template. Both steps require some practice.

This procedure routinely yielded arrays of microspheres on PDMS limited only by the resolution of the *i*-line photolithography (down to 0.5 μm holes in Si) used to generate the template, and by the limitations of hard contact between the spheres. The only defects we observed were point defects due to spheres that did not initially fill a templated position or did not transfer to the PDMS. We found this defect rate to be < 3%, with no other perceptible distortion to the transferred pattern of spheres. This defect mode occurred most likely due to the size variation in the spheres. Although our defect rate was low, we are confident that loading can be improved to >99% with more advanced filtering of the initial spheres to guarantee better monodispersity.

In the next phase of TEMPL (steps v-vii in Figure 1a) we used the templated microspheres as microlenses for projection photolithography.[15-17] Figure 1b shows a schematic description of the microlens projection lithography technique that we developed specifically for TEMPL. In more detail, we first prepared photosensitive substrates by spin-coating 200 nm of positive photoresist (from a diluted solution of Shipley S1805 in 1-methoxy-2-propyl acetate, see SI for the detailed experimental parameters) on the silicon substrates. We next coated these substrates with 1500 nm of poly(acrylic acid) (by spin-coating from an aqueous solution of PAA, see SI). The PAA layer formed a removable spacer[19] that set the focal plane of the microspheres to lie in the photoresist layer. We calculated the thickness of the PAA spacer based on an analytical model that we describe in the Supporting Information. We then brought the arrays of microspheres into direct contact with the PAA layer by carefully placing the PDMS slab (~ 1

mm thick; spheres side down) on top of the target substrate, and did not remove it until after the exposure with UV light.

To perform the patterning, we laser-cut macroscale masks into light-absorbing blackout paper, mounted a mask on a diffuser plate – to ensure homogenous illumination in all directions – 3 cm above the sample, and exposed with an intense, uncollimated, UV flood-light (450 mW/cm^2). After exposure, we removed the PDMS slab (including the spheres) manually, removed the PAA layer with water and developed the patterned photoresist using a conventional photoresist developer. Using this procedure, we routinely fabricated arrays of projected micropatterns with feature sizes down to 400 nm, with shapes determined by the macroscale mask, and with a spatial arrangement defined by the initial template. We include further details about methods, optical calculations, and our experimental set-up in the Supporting Information.

To demonstrate the applicability of TEMPL, we fabricated four different types of microlens arrays based on well-known, quasiperiodic structures: a Penrose lattice, a pinwheel lattice, and two different Vogel spirals (an α_1 spiral and a golden angle spiral).[4] These patterns provided useful test cases because they are complex, and known to exhibit interesting optical phenomena.[4, 10, 20-22] Figure 2 shows SEM images of three arrays of nanopatterns etched into photoresist after projection through three different nonperiodic arrays of microspheres. The sharpness of the Fourier transforms (Fig. 2d-f) of the images of the arrays shown in Fig. 2a-c confirms the high quality of these patterns.

Figure 3 shows a close-up view of these arrays and demonstrates the quality of the high-resolution nanopatterns obtained locally under each microsphere. The exposure time had to be optimized for every mask but since the process only takes a few seconds, and since the microlens arrays can be re-used, we did not find it to be a limiting factor.

We next demonstrate the use of TEMPL to produce structures active in the near infrared.

Figure 3d shows the simple T-structure that we chose for the unit cell. We prepared four different nonperiodic metasurfaces with TEMPL and then performed a standard lift-off procedure to metallize the patterns into gold. To simplify infrared optical measurements, we made some minor modifications to the fabrication process. Specifically, we i) used calcium fluoride disks for the target substrate; ii) spin-coated a lift-off resin onto the substrates before coating the photoresist; then, after development, iii) used electron beam deposition to lay down an adhesion layer of Ti (5 nm) followed by an active layer of Au (50 nm); and finally, iv) performed lift-off in warm (~80 °C) N-methylpyrrolidone. Figure 4b-e shows the resulting patterns.

We characterized these nonperiodic nanostructure arrays with an FTIR spectrometer and performed simulations by finite integration technique in CST microwave studio (see SI for details about the simulation). Because the global patterns were too complex to simulate, we only simulated spectra for a single unit cell. The measured spectra all showed a primary peak (both transmission and reflection) around 10 μm (Fig. 4g-j). Those spectra matched closely with the theoretical spectra (Fig. 4f). Slight differences in the position and depth of the peak were likely affected by the global symmetries of the lattices (or lack thereof). The reflectance was weaker than the transmittance, most likely due to loss by the rough top-surface of the nanoantennas. The Penrose and pinwheel lattices provide a stronger signal than the Vogel spirals, likely because of the higher overall areal density of the Penrose and pinwheel lattices.

Finally, to further demonstrate the broad applicability of TEMPL, and in particular the capability of fabricating high aspect ratio structures, we performed a deep reactive ion etching step on three metallized samples fabricated on silicon (where the metallic patterns thus served as an etch mask). We used a Bosch etch process[23] that was calibrated to achieve a 10 μm deep etching of silicon. The resulting non-periodic arrays of metal-capped vertical structures are

shown in Figure 5.

Overall, TEMPL enables rapid and inexpensive fabrication of large area arrays of arbitrarily positioned nanostructures. When using an unfiltered flood UV-source, the minimum feature size obtained with the microlenses we used was ~ 0.4 μm. TEMPL enables efficient exploration of the effect of lattice structure on the optical properties of infrared metasurfaces and allows the preparation of both periodic and non-periodic structures. Moreover, combined with deep reactive ion etching, TEMPL makes it possible to prepare high aspect ratio features and is therefore suited for the preparation of multilayer stacks as needed, for example, for the fabrication of zero-index metamaterials.[24, 25] This method may also enable the rapid fabrication of perfect absorbers for the IR range, with important applications to manufacturing efficient IR optics.[26] TEMPL may also be adapted to non-optical applications, as a convenient, alternative method for fabricating nanostructures with feature-sizes ranging between 0.4 –5 μm. Possibilities for further development include the use of superlens layers,[27, 28] which may open the door to super-resolution imaging with spherical microlenses.[29]

ACKNOWLEDGEMENTS

We thank A. A. Stokes, R. Nunes, and Ozge Akbulut for useful discussions. This work was supported by the Office of Naval Research under award no. N00014-10-1-0942. MG acknowledges Marie Curie award SAM-TunEGaIn:IOF-2012-328412. MH acknowledges Marie Curie IOF FP7 project nanoPAD (Grant Agreement Number 330017) the Bo Rydins stiftelse (SCA AB), and the Sweden-America Foundation. LR was funded by the REU program under National Science Foundation (NSF) under award No. DMR-1420570. This work was performed in part at the Center for Nanoscale Systems (CNS), a member of the National Nanotechnology Infrastructure Network (NNIN), which was supported by NSF award no. ECS-0335765. CNS is part of Harvard University.

REFERENCES

(1) Kildishev, A. V.; Boltasseva, A.; Shalaev, V. M. *Science* **2013**, *339*, 1289.

(2) Holloway, C. L.; Kuester, E. F.; Gordon, J. A.; O'Hara, J.; Booth, J.; Smith, D. R. *IEEE Antennas Propag. Mag.* **2012**, *54*, 10-35.

(3) Jahani, S.; Jacob, Z. *Nat. Nanotechnol.* **2016**, *11*, 23-36.

(4) Dal Negro, L.; Boriskina, S. V. *Laser Photonics Rev.* **2012**, *6*, 178-218.

(5) Lipworth, G.; Ensworth, J.; Seetharam, K.; Da, H.; Lee, J. S.; Schmalenberg, P.; Nomura, T.; Reynolds, M. S.; Smith, D. R.; Urzhumov, Y. *Sci. Rep.* **2014**, *4*, 3642.

(6) Yanik, A. A.; Cetin, A. E.; Huang, M.; Artar, A.; Mousavi, S. H.; Khanikaev, A.; Connor, J. H.; Shvets, G.; Altug, H. *Proc. Natl. Acad. Sci. U.S.A.* **2011**, *108*, 11784-11789.

(7) Xu, X.; Peng, B.; Li, D.; Zhang, J.; Wong, L. M.; Zhang, Q.; Wang, S.; Xiong, Q. *Nano Lett.* **2011**, *11*, 3232-3238.

(8) Wu, C.; Khanikaev, A. B.; Adato, R.; Arju, N.; Yanik, A. A.; Altug, H.; Shvets, G. *Nat. Mater.* **2012**, *11*, 69-75.

(9) Kravets, V. G.; Schedin, F.; Jalil, R.; Britnell, L.; Gorbachev, R. V.; Ansell, D.; Thackray, B.; Novoselov, K. S.; Geim, A. K.; Kabashin, A. V., et al. *Nat. Mater.* **2013**, *12*, 304-309.

(10) Dal Negro, L. *SPIE Newsroom* **2012**, DOI: 10.1117/2.1201206.004306.

(11) Xie, L.; Gao, W.; Shu, J.; Ying, Y.; Kono, J. *Sci. Rep.* **2015**, *5*, 8671.

(12) Aieta, F.; Genevet, P.; Kats, M. A.; Yu, N.; Blanchard, R.; Gaburro, Z.; Capasso, F. *Nano Lett.* **2012**, *12*, 4932-4936.

(13) Yu, N.; Capasso, F. *Nat. Mater.* **2014**, *13*, 139-150.

(14) Lin, D.; Fan, P.; Hasman, E.; Brongersma, M. L. *Science* **2014**, *345*, 298-302.

(15) Wu, M.-H.; Whitesides, G. M. *Appl. Phys. Lett.* **2001**, *78*, 2273-2275.

(16) Wu, M.-H.; Whitesides, G. M. *J. Micromech. Microeng.* **2002**, *12*, 747-758.

(17) Wu, M.-H.; Park, C.; Whitesides, G. M. *J. Colloid Interface Sci.* **2003**, *265*, 304-309.

(18) Khanh, N. N.; Yoon, K. B. *J. Am. Chem. Soc.* **2009**, *131*, 14228-14230.

(19) Linder, V.; Gates, B. D.; Ryan, D.; Parviz, B. A.; Whitesides, G. M. *Small* **2005**, *1*, 730-736.

(20) Dal Negro, L., *Optics of aperiodic structures : fundamentals and device applications*. Pan Stanford: Singapore, 2014.

(21) Dal Negro, L.; Lawrence, N.; Trevino, J., Engineering Aperiodic Spiral Order in Nanophotonics: Fundamentals and Device Applications. In *Nanodevices for Photonics and Electronics*, Bettotti, P., Ed. Pan Stanford: Singapore, 2015; pp. 57-125.

(22) Dal Negro, L.; Lawrence, N.; Trevino, J., Engineering the Orbital Angular Momentum of Light with Plasmonic Vogel Spiral Arrays. In *Singular and Chiral Nanoplasmonics*, Boriskina, S.; Zheludev, N. I., Eds. Pan Stanford: Singapore, 2014; pp. 335-374.

(23) Laermer, F.; Schilp, A. Method of anisotropically etching silicon. U.S. Patent 5,501,893, 1996.

(24) Li, Y.; Kita, S.; Muñoz, P.; Reshef, O.; Vulis, D. I.; Yin, M.; Lončar, M.; Mazur, E. *Nat. Photonics* **2015**, *9*, 738-742.

(25) Moitra, P.; Yang, Y.; Anderson, Z.; Kravchenko, I. I.; Briggs, D. P.; Valentine, J. *Nat. Photonics* **2013**, *7*, 791-795.

(26) Liu, N.; Mesch, M.; Weiss, T.; Hentschel, M.; Giessen, H. *Nano Lett.* **2010**, *10*, 2342-2348.

(27) Fang, N.; Lee, H.; Sun, C.; Zhang, X. *Science* **2005**, *308*, 534-537.

(28) Zhang, X.; Liu, Z. *Nat. Mater.* **2008**, *7*, 435-441.

(29) Li, S.; Du, C.; Dong, X.; Shi, L.; Luo, X.; Wei, X.; Zhang, Y. *Opt. Express* **2008**, *16*, 14397-14403.

Figure 1. Schematic diagram of the templated microlens process flow (A) from the template in silicon to the final substrate. i) the holes in the silicon wafer are filled with PEI, ii) the beads are selectively adhered inside the holes due to their adhesion to PEI, iii) the PEI is removed by thermal decomposition with a butane torch, iv) the beads are picked-up with a PDMS slab, v) the array of beads is placed in contact with the substrate, vi) the exposure is performed through the PDMS and the spheres, and the sample is developed, vii) the pattern is transferred by metallization and lift off (a) or by etching (b). (B) Schematic diagram of the projection lithography setup. An intense source of non-collimated UV-light impinges on the cm-scale photomask, and the transmitted light is focused by the lensing of each microsphere onto the underlying photoresist to create a replica of the features of the mask.

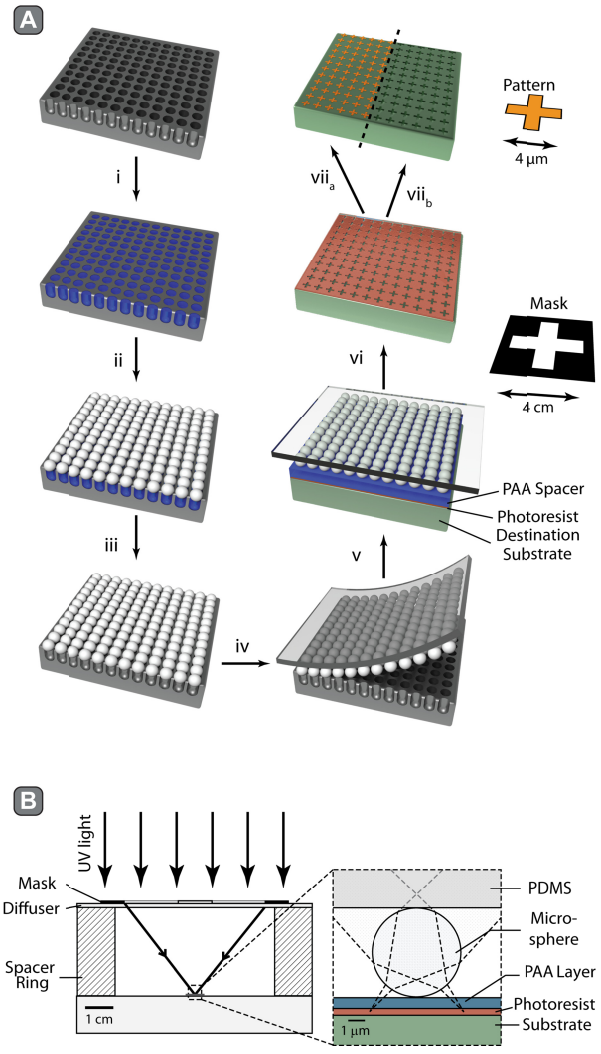

Figure 2. SEM micrograph of three different sample arrays fabricated by TEMPL, showing an α_1-spiral lattice (A), a pinwheel lattice (B), and a Penrose lattice (C). The Fourier transform of the SEM images (D-F), show the overall quality of the non-periodic lattice structures. Figure 3 shows SEM images of the same samples at a higher magnification.

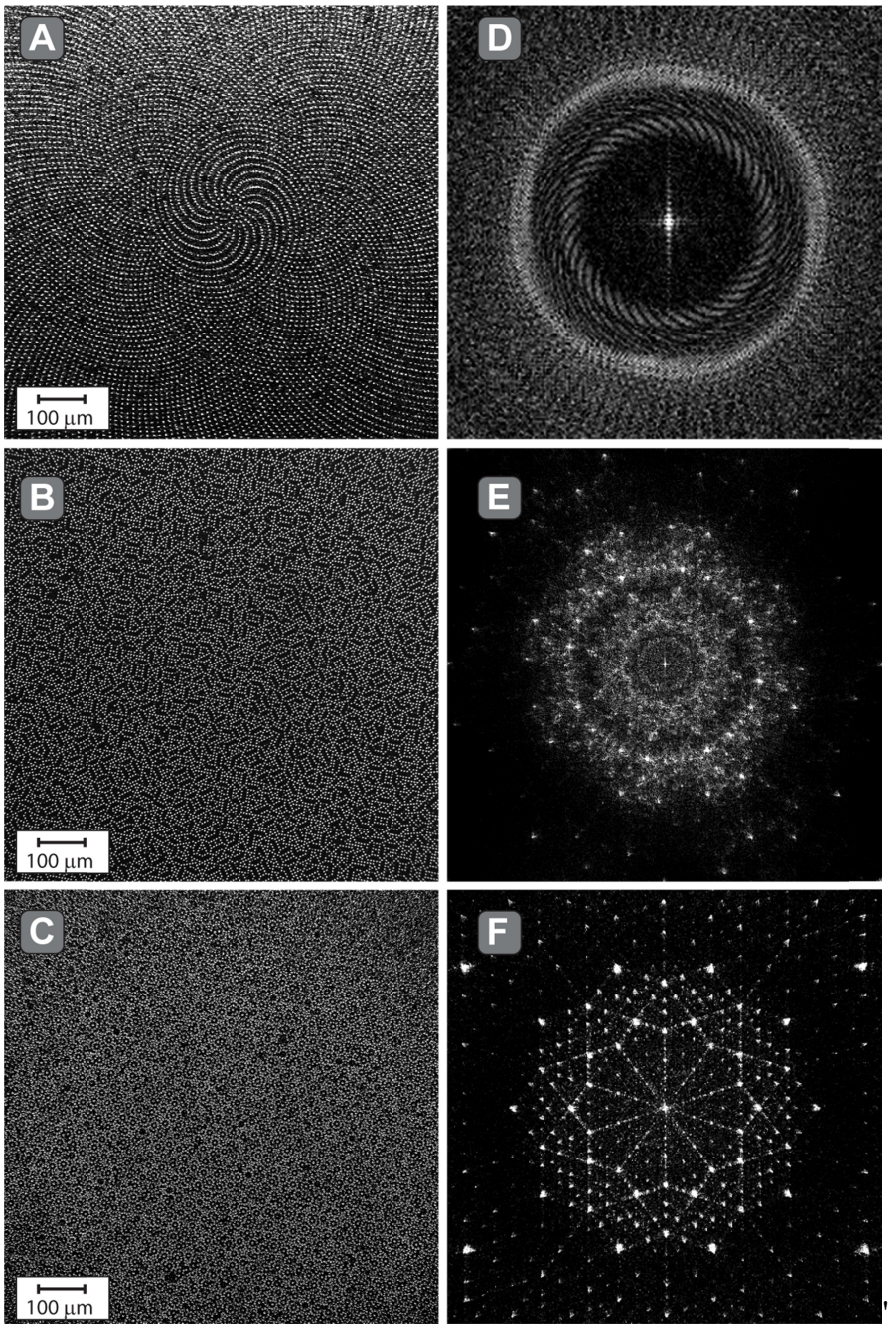

Figure 3. Enlarged SEM micrograph of the three samples from Fig. 2, showing an α_1-spiral (A) lattice of T patterns (D), a pinwheel lattice (B) of chiral triskel patterns (E), and a Penrose lattice (C) of split C resonator patterns (D).

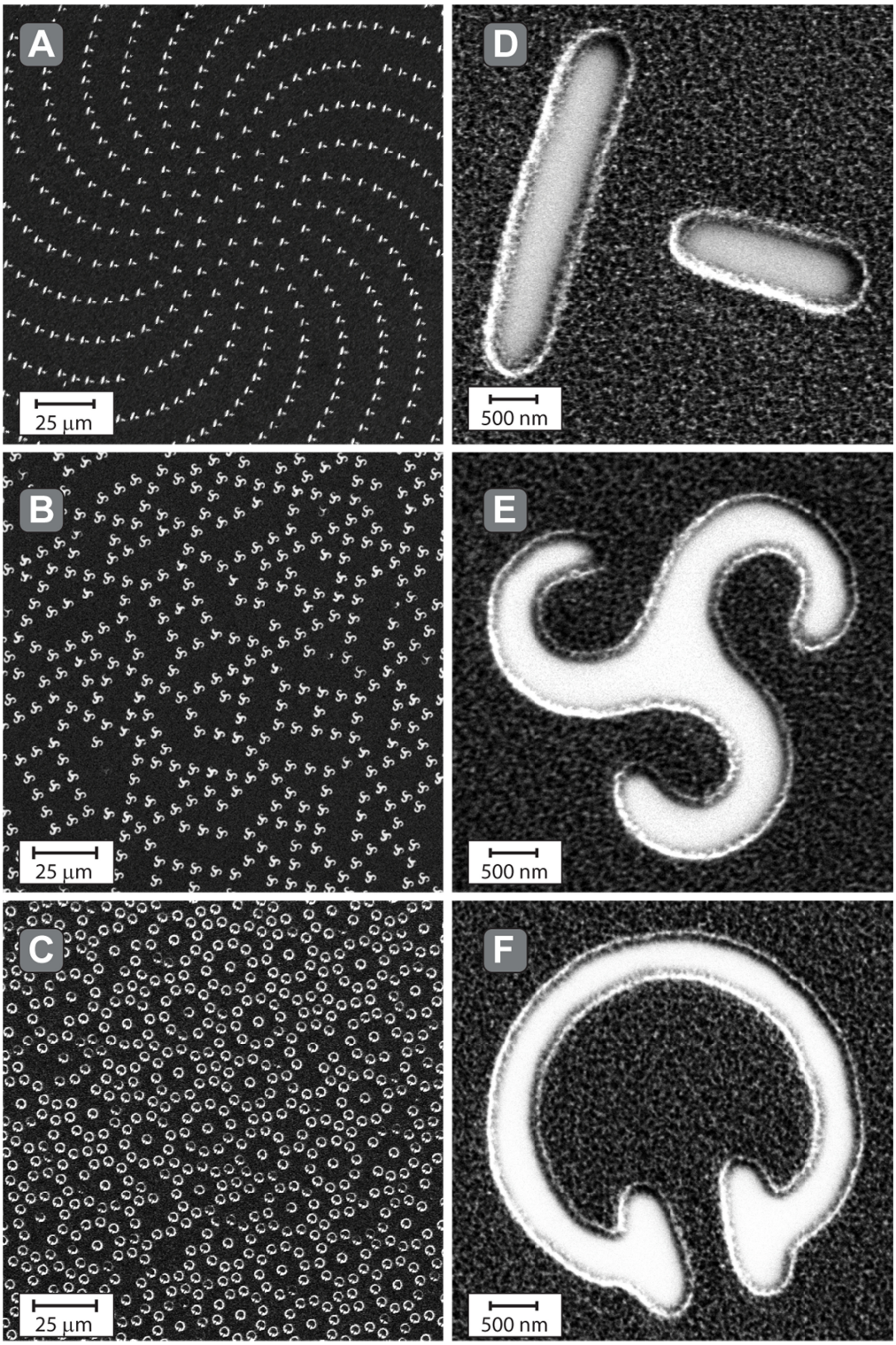

Figure 4. (top row left) schematic diagram of single t-shaped nano patterns. (top row right) theoretical transmittance and reflectance IR spectra for the single T-shape pattern. SEM micrographs (left), and optical transmittance and reflectance IR spectra (right), for four different arrays of gold T-shaped nanopatterns fabricated on CaF_2.

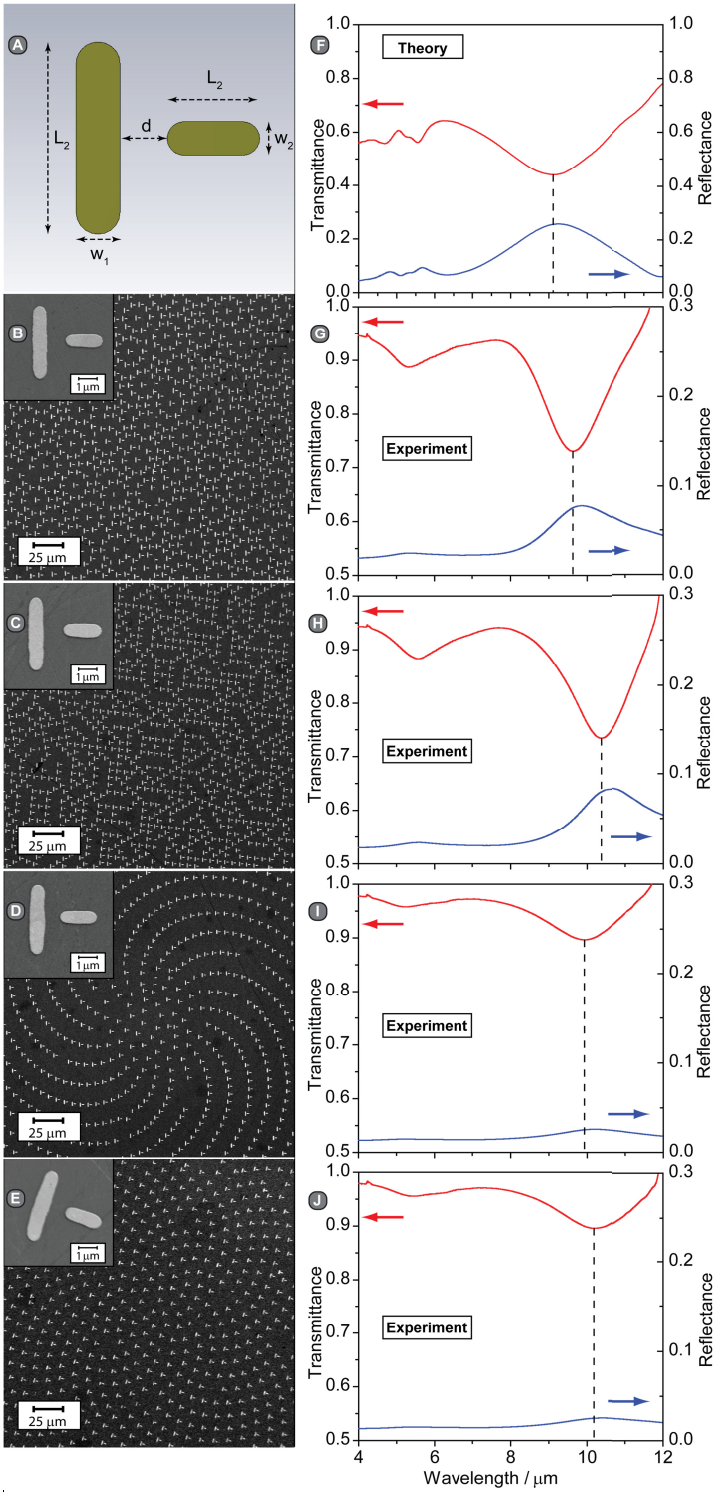

Figure 5. A T-shaped nano pattern that was first patterned in gold on silicon and then etched to yield micro-pillars using DRIE. The different lattice structures are an α_1 spiral (a) and (d), a Penrose lattice (b) and (e), and a pinwheel lattice (c) and (f).